

Measurements of $B \rightarrow DK$ decays to constrain the CKM
Unitarity Triangle angle γ and related results at LHCbDANIEL CRAIK ¹*Department of Physics
University of Warwick, Coventry, UK*

Constraints on the CKM angle γ are presented from GLW, ADS, and GGSZ analyses of $B^\pm \rightarrow DK^\pm$ at the LHCb experiment. The branching fractions of $B^0 \rightarrow \bar{D}^0 K^+ \pi^-$ and $B_s^0 \rightarrow \bar{D}^0 K^- \pi^+$ are also reported, measured relative to the related mode $B^0 \rightarrow \bar{D}^0 \pi^+ \pi^-$.

PRESENTED AT

DPF 2013

The Meeting of the American Physical Society
Division of Particles and Fields
Santa Cruz, California, August 13–17, 2013

¹On behalf of the LHCb Collaboration.

1 Measurements of γ from $B^\pm \rightarrow DK^\pm$

The CKM angle $\gamma = \arg(-V_{ud}V_{ub}^*/V_{cd}V_{cb}^*)$ is currently the least well-constrained angle in the Unitarity Triangle. So far, the most-sensitive measurements of γ from a single experiment have been performed by Belle [1] and BaBar [2]. These measurements yield values of $(68^{+15}_{-14})^\circ$ and $(69^{+17}_{-16})^\circ$, respectively.

Tree-level processes such as $B^\pm \rightarrow DK^\pm$ provide a theoretically clean measurement of γ with no contributions from new physics processes. This measurement can be compared with measurements from loop-mediated processes, which are sensitive to new physics, to provide a test of the Standard Model. The current limits on the CKM Unitarity Triangle due to tree-level and loop processes, as calculated by the CKMFitter group [3], are shown in Fig. 1.

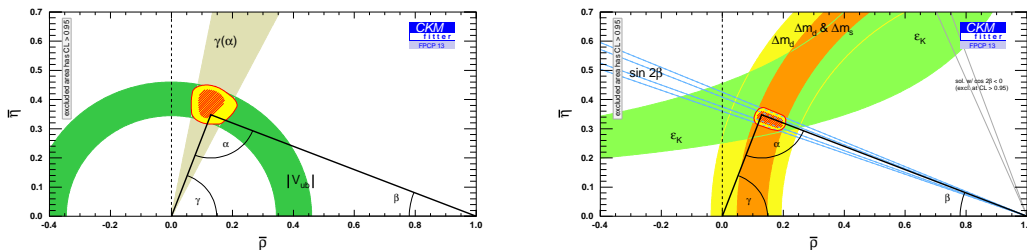


Figure 1: Constraints on the CKM Unitarity Triangle due to (left) tree-level processes and (right) loop-mediated processes.

1.1 GLW/ADS analysis of $B^\pm \rightarrow DK^\pm$ and $B^\pm \rightarrow D\pi^\pm$

The GLW method [4] uses D decays to CP eigenstates such as K^+K^- and $\pi^+\pi^-$. Decays can proceed either via a D^0 or a \bar{D}^0 with a phase difference of $\delta_B + \gamma$. Suppression in the decay via D^0 with respect to the \bar{D}^0 decay limits interference to $\mathcal{O}(10\%)$ in $B^\pm \rightarrow DK^\pm$ and $\mathcal{O}(1\%)$ in $B^\pm \rightarrow D\pi^\pm$.

The ADS method [5] uses D decays to quasi-flavour-specific states such as π^+K^- and $\pi^-K^+\pi^+\pi^-$. Here the suppression of one of the B decays is partially balanced by the suppression of one of the D decays, giving larger interference terms while also introducing an additional phase shift of δ_D .

Analyses have been performed on $B^\pm \rightarrow DK^\pm$ and $B^\pm \rightarrow D\pi^\pm$ with the D meson reconstructed from the final states K^+K^- , $\pi^+\pi^-$, $K^+\pi^-$, π^+K^- , $K^-\pi^+\pi^+\pi^-$ and $\pi^-K^+\pi^+\pi^-$ using LHCb data corresponding to 1fb^{-1} of pp collisions at a centre of mass energy of 7 TeV [6, 7]. The invariant mass distributions of the two- and four-body suppressed ADS modes are shown in Fig. 2 and Fig. 3, respectively. The

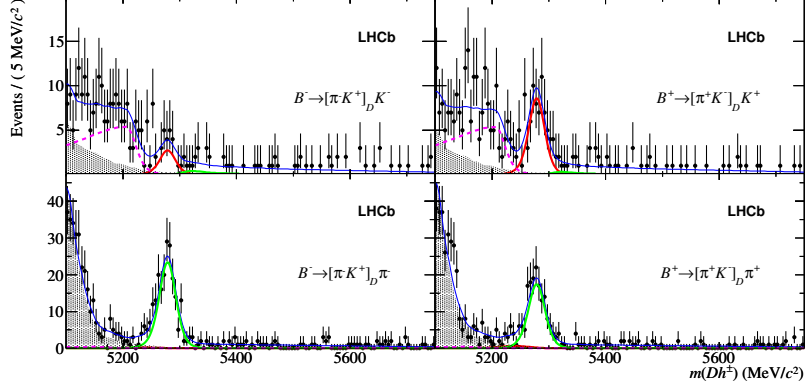


Figure 2: Fits to the invariant mass distributions of the two-body suppressed ADS mode $\pi^\mp K^\pm$ in (top) $B^\mp \rightarrow DK^\mp$ and (bottom) $B^\mp \rightarrow D\pi^\mp$. The $B^\mp \rightarrow DK^\mp$ and $B^\mp \rightarrow D\pi^\mp$ components are shown in red and green, respectively. The shaded component indicates partially reconstructed background, the dashed magenta line corresponds to partially reconstructed $\Lambda_c^0 \rightarrow \Lambda_c^+ h^-$ and the total shape also includes a combinatoric background.

observables measured are the ratio of DK to $D\pi$ for each D final state,

$$R_{K/\pi}^f = \frac{\Gamma(B^- \rightarrow D[\rightarrow f]K^-) + \Gamma(B^+ \rightarrow D[\rightarrow \bar{f}]K^+)}{\Gamma(B^- \rightarrow D[\rightarrow f]\pi^-) + \Gamma(B^+ \rightarrow D[\rightarrow \bar{f}]\pi^+)},$$

the charge asymmetry for each final state,

$$A_h^f = \frac{\Gamma(B^- \rightarrow D[\rightarrow f]h^-) - \Gamma(B^+ \rightarrow D[\rightarrow \bar{f}]h^+)}{\Gamma(B^- \rightarrow D[\rightarrow f]h^-) + \Gamma(B^+ \rightarrow D[\rightarrow \bar{f}]h^+)},$$

and the ratio of the suppressed to favoured modes for $D \rightarrow K\pi$ and $D \rightarrow K\pi\pi$,

$$R_h^\pm = \frac{B^\pm \rightarrow D[f_{\text{sup}}]h^\pm}{B^\pm \rightarrow D[f]h^\pm}.$$

The values obtained for each of these observables can be found in Refs. [6, 7]. These variables serve as inputs for the combined γ measurements in Section 1.3 and Section 1.4.

1.2 GGSZ analysis of $B^\pm \rightarrow DK^\pm$

The GGSZ method [8] exploits the variation of the strong phase δ_D across the Dalitz plot in D decays to three-body self-conjugate states such as $K_S^0\pi^+\pi^-$ and $K_S^0K^+K^-$. The Dalitz plot is divided into bins, as shown in Fig. 4, chosen to maximise statistical sensitivity. The populations of B^+ and B^- decays in each bin are given by

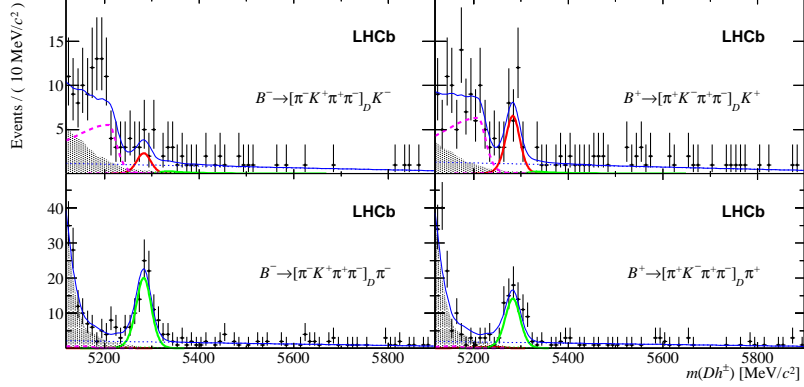


Figure 3: Fits to the invariant mass distributions of the four-body suppressed ADS mode $\pi^\mp K^\pm \pi^\pm \pi^\mp$ in (top) $B^\mp \rightarrow DK^\mp$ and (bottom) $B^\mp \rightarrow D\pi^\mp$. The $B^\mp \rightarrow DK^\mp$ and $B^\mp \rightarrow D\pi^\mp$ components are shown in red and green, respectively. The shaded component indicates partially reconstructed background, the dashed magenta line corresponds to partially reconstructed $B_s^0 \rightarrow DK^- \pi^+$ and the total shape also includes a combinatoric background.

$$N_{\pm i}^+ = h_{B^+} \left[K_{\mp i} + (x_+^2 + y_+^2) K_{\pm i} + 2\sqrt{K_i K_{-i}} (x_+ c_{\pm i} \mp y_+ s_{\pm i}) \right],$$

$$N_{\pm i}^- = h_{B^-} \left[K_{\pm i} + (x_-^2 + y_-^2) K_{\mp i} + 2\sqrt{K_i K_{-i}} (x_- c_{\pm i} \pm y_- s_{\pm i}) \right],$$

where $K_{\pm i}$ is the efficiency corrected yield in bin $\pm i$ due to D^0 flavour tagged events from BaBar [9, 10] and $c_{\pm i}$ and $s_{\pm i}$ are the cosine and sine of the strong phase δ_D in bin $\pm i$ from CLEO-c [11].

The remaining parameters are left free in the fit to the data: h_{B^\pm} are normalisation factors for B^\pm , and $x_\pm = r_B \cos(\delta_B \pm \gamma)$ and $y_\pm = r_B \sin(\delta_B \pm \gamma)$ are the Cartesian parameters, which are sensitive to γ .

Analyses have been performed on $B^\pm \rightarrow DK^\pm$ with the D meson reconstructed in the final states $K_S^0 \pi^+ \pi^-$ and $K_S^0 K^+ K^-$ using LHCb data corresponding to 1 fb^{-1} of pp collisions at a centre of mass energy of 7 TeV [12] and 2 fb^{-1} of pp collisions at a centre of mass energy of 8 TeV [13]. The values obtained for the Cartesian parameters in the 8 TeV analysis are

$$x_+ = (-8.7 \pm 3.1(\text{stat.}) \pm 1.6(\text{syst.}) \pm 0.6(\text{ext.})) \times 10^{-2},$$

$$x_- = (5.3 \pm 3.2(\text{stat.}) \pm 0.9(\text{syst.}) \pm 0.9(\text{ext.})) \times 10^{-2},$$

$$y_+ = (0.1 \pm 3.6(\text{stat.}) \pm 1.4(\text{syst.}) \pm 1.9(\text{ext.})) \times 10^{-2},$$

$$y_- = (9.9 \pm 3.6(\text{stat.}) \pm 2.2(\text{syst.}) \pm 1.6(\text{ext.})) \times 10^{-2},$$

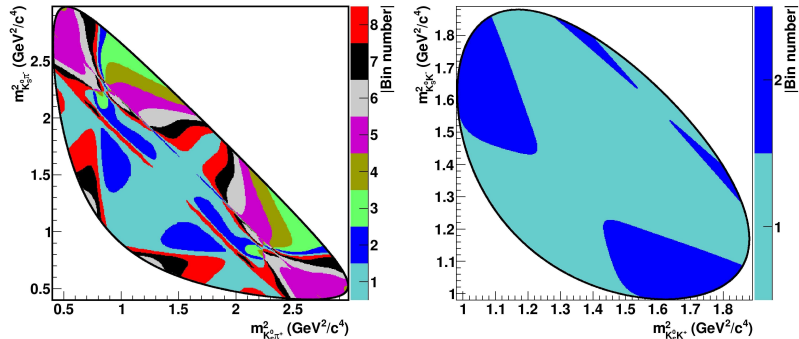


Figure 4: Binning schemes used for the Dalitz plots of (left) $D \rightarrow K_S^0 \pi^+ \pi^-$ and (right) $D \rightarrow K_S^0 K^+ K^-$. Bins in the top-left half of the plots ($m_{K_S^0 h^-}^2 > m_{K_S^0 h^+}^2$) are identified as $+i$ and bins in the bottom-right half are labeled $-i$.

where the third uncertainty is due to the CLEO-c strong phase measurements used in the fit.

Combining these values with the results from the 7 TeV analysis and fitting for γ , r_B and δ_B yields values of $(57 \pm 16)^\circ$, $(8.8_{-2.4}^{+2.3}) \times 10^{-2}$ and $(124_{-17}^{+15})^\circ$, respectively, where the values for γ and δ_B are modulo 180° . Two-dimensional projections of the confidence regions for these parameters are shown in Fig. 5.

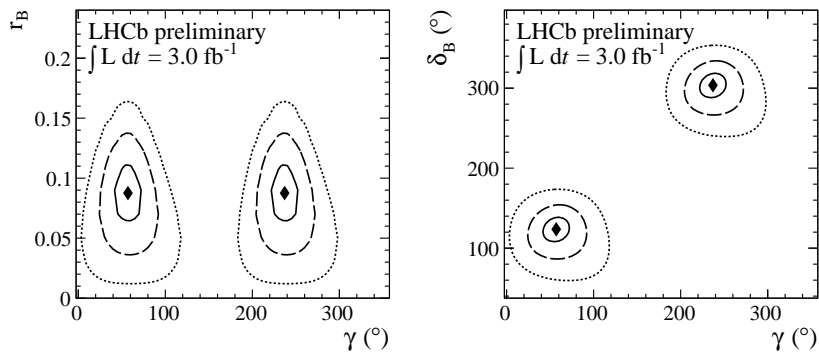


Figure 5: Two-dimensional projections of the confidence regions onto the (left) (γ, r_B) and (right) (γ, δ_B) planes. Contours indicate the 1, 2 and 3σ boundaries and diamonds mark the central values.

1.3 Combination of results from 1 fb^{-1} measurements

The results in Section 1.1 and Section 1.2 are combined using a frequentist approach to obtain a more constraining measurement of γ [14]. In addition to these results

combination	γ	68 % CL	95 % CL
DK	72.0°	$[56.4, 86.7]^\circ$	$[42.6, 99.6]^\circ$
$D\pi$	18.9°	$[7.4, 99.2]^\circ \cup [167.9, 176.4]^\circ$	-
DK and $D\pi$	72.6°	$[55.4, 82.3]^\circ$	$[40.2, 92.7]^\circ$

Table 1: Best-fit values and confidence intervals for γ from the combination of DK and $D\pi$ measurements.

further measurements are included to improve the fit: measurements of the strong phases and coherence factors for $D \rightarrow K\pi$ and $D \rightarrow K\pi\pi\pi$ decays from CLEO-c [15], CP asymmetry measurements of the neutral D mesons from the Heavy Flavour Averaging Group [16] and charm mixing parameters from LHCb [17]. A likelihood is constructed from the measured observables as

$$\mathcal{L}(\vec{\alpha}) = \prod_i \xi_i \left(\vec{A}_i^{\text{obs}} | \vec{\alpha} \right),$$

where the sum is over the different measurements, $\vec{\alpha}$ is the set of parameters and ξ_i denotes the likelihood probability density functions (PDFs) of the observables \vec{A}_i^{obs} . For most observables a Gaussian PDF is assumed, however, where highly non-Gaussian behaviour is observed, the experimental likelihood is used.

A combined γ measurement has been performed including the results from Section 1.1 and a subset of the results from Section 1.2 corresponding to 1 fb^{-1} of pp collisions at a centre of mass energy of 7 TeV [12]. The best-fit values and confidence intervals (modulo 180°) of γ are given in Table 1 and the $1 - \text{CL}$ curves for γ are shown in Fig. 6.

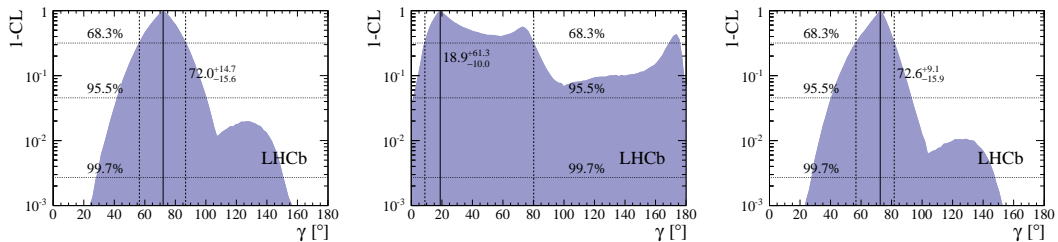


Figure 6: $1 - \text{CL}$ curves for γ from the combined 1 fb^{-1} GLW/ADS and 1 fb^{-1} GGSZ measurements using (left) only DK , (centre) only $D\pi$ and (right) both decay modes.

1.4 Combination including 3 fb^{-1} GGSZ measurement

Another combination [18] has been performed that incorporates all of the results reported in Section 1.2 but only those observables from Section 1.1 corresponding

quantity	value	68 % CL	95 % CL
γ	67.2°	$[55.1, 79.1]^\circ$	$[43.9, 89.5]^\circ$
r_B	0.0923	$[0.0843, 0.1001]$	$[0.0762, 0.1075]$
δ_B	114.3°	$[101.3, 126.3]^\circ$	$[88.7, 136.3]^\circ$

Table 2: Best-fit values and confidence intervals for γ , r_B and δ_B from the combination of DK measurements including GGSZ measurements from 3 fb^{-1} of data.

to $B^\pm \rightarrow DK^\pm$ decays. Mixing in the neutral D mesons is also neglected in the equations used for the observables in this combination.

The best-fit values and confidence intervals (all modulo 180°) for γ , r_B and δ_B are given in Table 2. Figure 7 and Figure 8 show the $1 - \text{CL}$ curve for γ , and the 2D projection of the likelihood in γ and r_B , respectively.

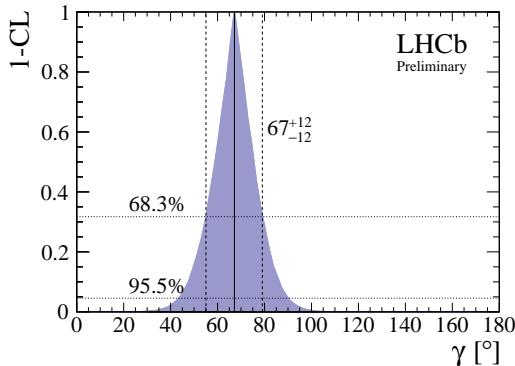


Figure 7: $1 - \text{CL}$ curve for γ from the combined 1 fb^{-1} GLW/ADS and 3 fb^{-1} GGSZ measurements.

2 Measurement of $B_{(s)}^0 \rightarrow DK\pi$ branching fractions

The decay mode $B^0 \rightarrow DK^+\pi^-$ has potential for a significant future measurement of γ [19–21]. Sensitivity to γ comes from the interference of $b \rightarrow c$ and $b \rightarrow u$ amplitudes of a similar magnitude. $B_s^0 \rightarrow DK^-\pi^+$ and the related mode $B_s^0 \rightarrow D^*K^-\pi^+$ form important backgrounds to this mode, therefore, an understanding of these modes is necessary.

Branching fraction measurements of $B^0 \rightarrow DK^+\pi^-$ and $B_s^0 \rightarrow DK^-\pi^+$, relative to the normalisation mode $B^0 \rightarrow D\pi^+\pi^-$, have been made using LHCb data corresponding to 1 fb^{-1} of pp collisions at a centre of mass energy of 7 TeV [22].

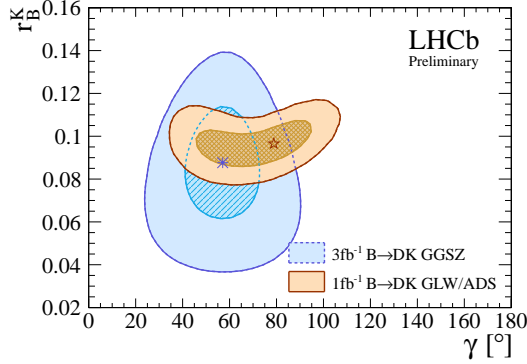


Figure 8: Two-dimensional projection of the confidence regions onto the (γ, r_B) plane. Contours show the 1 and 2σ boundaries and markers indicate the central values.

The invariant mass distributions of $D\pi\pi$ and $DK\pi$ candidates where the D is reconstructed from $\bar{D}^0 \rightarrow K^+\pi^-$ are shown in Fig. 9. The measured relative branching fractions are

$$\frac{\mathcal{B}(B^0 \rightarrow \bar{D}^0 K^+ \pi^-)}{\mathcal{B}(B^0 \rightarrow \bar{D}^0 \pi^+ \pi^-)} = 0.106 \pm 0.007 (\text{stat.}) \pm 0.008 (\text{syst.}),$$

$$\frac{\mathcal{B}(B_s^0 \rightarrow \bar{D}^0 K^- \pi^+)}{\mathcal{B}(B^0 \rightarrow \bar{D}^0 \pi^+ \pi^-)} = 1.18 \pm 0.05 (\text{stat.}) \pm 0.12 (\text{syst.}).$$

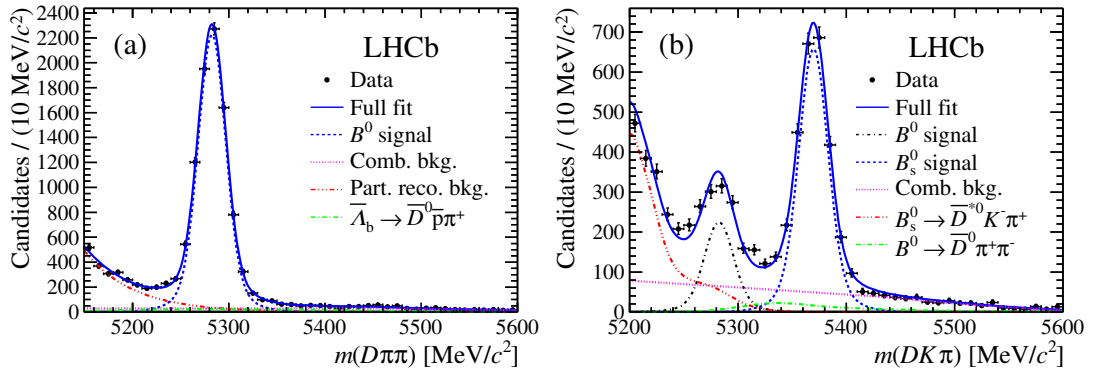


Figure 9: Fits to the $B_{(s)}^0$ candidate invariant mass distributions for the (a) $D\pi\pi$ and (b) $DK\pi$ samples. Data points are shown in black, the full fitted PDFs as solid blue lines and the components as detailed in the legends.

These relative measurements yield absolute branching fractions of

$$\mathcal{B}(B^0 \rightarrow \bar{D}^0 K^+ \pi^-) = (9.0 \pm 0.6 \text{ (stat.)} \pm 0.7 \text{ (syst.)} \pm 0.9(\mathcal{B})) \times 10^{-5},$$

$$\mathcal{B}(B_s^0 \rightarrow \bar{D}^0 K^- \pi^+) = (1.00 \pm 0.04 \text{ (stat.)} \pm 0.10 \text{ (syst.)} \pm 0.10(\mathcal{B})) \times 10^{-3},$$

where the third uncertainty arises from the uncertainties on $\mathcal{B}(B^0 \rightarrow \bar{D}^0 \pi^+ \pi^-)$. This is the most precise measurement of $\mathcal{B}(B^0 \rightarrow \bar{D}^0 K^+ \pi^-)$ to date and the first measurement of $\mathcal{B}(B_s^0 \rightarrow \bar{D}^0 K^- \pi^+)$.

Although no quantitative analysis of the Dalitz plots has yet been attempted, the Dalitz plot distributions obtained (corrected for efficiency) are presented in Fig. 10.

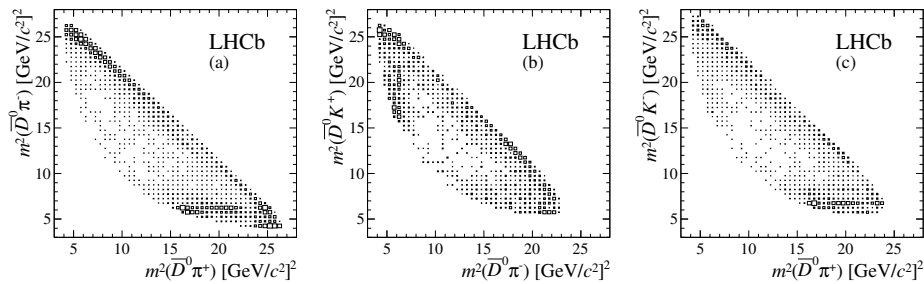


Figure 10: Efficiency corrected Dalitz plot distributions for (a) $B^0 \rightarrow \bar{D}^0 \pi^+ \pi^-$, (b) $B^0 \rightarrow \bar{D}^0 K^+ \pi^-$ and (c) $B_s^0 \rightarrow \bar{D}^0 K^- \pi^+$ candidates obtained from the signal weights.

3 Conclusions and prospects

The $B^\pm \rightarrow DK^\pm$ decay mode offers an excellent opportunity to measure the CKM angle γ from Standard Model processes. The combination in Section 1.4 gives the most sensitive measurement of γ from a single experiment so far, yielding a value of $(67 \pm 12)^\circ$. This measurement is expected to improve further with the completion of a GLW/ADS analysis on the remaining 2 fb^{-1} of LHCb data currently available. In addition, other modes such as $B^0 \rightarrow DK^+ \pi^-$ offer great prospects for future γ measurements.

ACKNOWLEDGMENTS

This work is funded in part by the European Research Council under FP7 and by the United Kingdom's Science and Technology Facilities Council.

References

- [1] K. Trabelsi [Belle Collaboration], arXiv:1301.2033 [hep-ex].
- [2] J. P. Lees *et al.* [BaBar Collaboration], Phys. Rev. D **87** (2013) 052015 [arXiv:1301.1029 [hep-ex]].
- [3] J. Charles *et al.* [CKMfitter Group Collaboration], Eur. Phys. J. C **41** (2005) 1 [hep-ph/0406184].
- [4] M. Gronau and D. Wyler, Phys. Lett. B **265** (1991) 172.
- [5] D. Atwood, I. Dunietz and A. Soni, Phys. Rev. Lett. **78** (1997) 3257 [hep-ph/9612433].
- [6] R. Aaij *et al.* [LHCb Collaboration], Phys. Lett. B **712** (2012) 203 [Erratum-ibid. B **713** (2012) 351] [arXiv:1203.3662 [hep-ex]].
- [7] R. Aaij *et al.* [LHCb Collaboration], Phys. Lett. B **723** (2013) 44 [arXiv:1303.4646 [hep-ex]].
- [8] A. Giri, Y. Grossman, A. Soffer and J. Zupan, Phys. Rev. D **68** (2003) 054018 [hep-ph/0303187].
- [9] B. Aubert *et al.* [BaBar Collaboration], Phys. Rev. D **78** (2008) 034023 [arXiv:0804.2089 [hep-ex]].
- [10] P. del Amo Sanchez *et al.* [BaBar Collaboration], Phys. Rev. Lett. **105** (2010) 121801 [arXiv:1005.1096 [hep-ex]].
- [11] J. Libby *et al.* [CLEO Collaboration], Phys. Rev. D **82** (2010) 112006 [arXiv:1010.2817 [hep-ex]].
- [12] R. Aaij *et al.* [LHCb Collaboration], Phys. Lett. B **718** (2012) 43 [arXiv:1209.5869 [hep-ex]].
- [13] R. Aaij *et al.* [LHCb Collaboration], LHCb-CONF-2013-004 (2013).
- [14] R. Aaij *et al.* [LHCb Collaboration], arXiv:1305.2050 [hep-ex].
- [15] N. Lowrey *et al.* [CLEO Collaboration], Phys. Rev. D **80** (2009) 031105 [arXiv:0903.4853 [hep-ex]].
- [16] Y. Amhis *et al.* [Heavy Flavor Averaging Group Collaboration], arXiv:1207.1158 [hep-ex].

- [17] R. Aaij *et al.* [LHCb Collaboration], Phys. Rev. Lett. **110** (2013) 101802 [arXiv:1211.1230 [hep-ex]].
- [18] R. Aaij *et al.* [LHCb Collaboration], LHCb-CONF-2013-006 (2013).
- [19] M. Gronau, Phys. Lett. B **557** (2003) 198 [hep-ph/0211282].
- [20] T. Gershon, Phys. Rev. D **79** (2009) 051301 [arXiv:0810.2706 [hep-ph]].
- [21] T. Gershon and M. Williams, Phys. Rev. D **80** (2009) 092002 [arXiv:0909.1495 [hep-ph]].
- [22] R. Aaij *et al.* [LHCb Collaboration], Phys. Rev. D **87** (2013) 112009 [arXiv:1304.6317 [hep-ex]].